Supercontinuum-based 10-GHz flat-topped optical frequency comb generation

Rui Wu,[1,*] Victor Torres-Company,[1,2] Daniel E. Leaird,[1] and Andrew M. Weiner[1]

[1]*School of Electrical and Computer Engineering, Purdue University, 465 Northwestern Avenue, West Lafayette, Indiana 47907, USA*

[2]*Currently with Microtechnology and Nanoscience Department, Chalmers University of Technology, SE-41296 Göteborg, Sweden*

[*]*rwu@purdue.edu*

Abstract: The generation of high-repetition-rate optical frequency combs with an ultra-broad, coherent and smooth spectrum is important for many applications in optical communications, radio-frequency photonics and optical arbitrary waveform generation. Usually, nonlinear broadening techniques of comb-based sources do not provide the required flatness over the whole available bandwidth. Here we present a 10-GHz ultra-broadband flat-topped optical frequency comb (> 3.64-THz or 28 nm bandwidth with ~365 spectral lines within 3.5-dB power variation) covering the entire C-band. The key enabling point is the development of a pre-shaping-free directly generated Gaussian comb-based 10-GHz pulse train to seed a highly nonlinear fiber with normal dispersion profile. The combination of the temporal characteristics of the seed pulses with the nonlinear device allows the pulses to enter into the optical wave-breaking regime, thus achieving a smooth flat-topped comb spectral envelope. To further illustrate the high spectral coherence of the comb, we demonstrate high-quality pedestal-free short pulse compression to the transform-limited duration.

OCIS codes: (060.4370) Nonlinear optics, fibers; (060.4510) Optical communications; (060.5060) Phase modulation; (060.5530) Pulse propagation and temporal solitons; (190.7110) Ultrafast nonlinear optics; (230.2090) Electro-optical devices; (320.5520) Pulse compression.

References and links

1. T. Morioka, K. Mori, and M. Saruwatari, "More than 100-wavelength-channel picosecond optical pulse generation from single laser source using supercontinuum in optical fibers," Electron. Lett. **29**(10), 862–864 (1993).
2. D. Hillerkuss, R. Schmogrow, T. Schellinger, M. Jordan, M. Winter, G. Huber, T. Vallaitis, R. Bonk, P. Kleinow, F. Frey, M. Roeger, S. Koenig, A. Ludwig, A. Marculescu, J. Li, M. Hoh, M. Dreschmann, J. Meyer, S. Ben Ezra, N. Narkiss, B. Nebendahl, F. Parmigiani, P. Petropoulos, B. Resan, A. Oehler, K. Weingarten, T. Ellermeyer, J. Lutz, M. Moeller, M. Huebner, J. Becker, C. Koos, W. Freude, and J. Leuthold, "26 Tbit s^{-1} line-rate super-channel transmission utilizing all-optical fast fourier transform processing," Nat. Photonics **5**(6), 364–371 (2011).
3. Z. Jiang, C. B. Huang, D. E. Leaird, and A. M. Weiner, "Optical arbitrary waveform processing of more than 100 spectral comb lines," Nat. Photonics **1**(8), 463–467 (2007).
4. T. J. Kippenberg, R. Holzwarth, and S. A. Diddams, "Microresonator-based optical frequency combs," Science **332**(6029), 555–559 (2011).
5. Z. Tong, A. O. Wiberg, E. Myslivets, B. P. Kuo, N. Alic, and S. Radic, "Spectral linewidth preservation in parametric frequency combs seeded by dual pumps," Opt. Express **20**(16), 17610–17619 (2012).
6. F. Ferdous, H. Miao, D. E. Learid, K. Srinivasan, J. Wang, L. Chen, L. T. Varghese, and A. M. Weiner, "Spectral line-by-line pulse shaping of on-chip microresonator frequency combs," Nat. Photonics **5**(12), 770–776 (2011).
7. S. Papp and S. Diddams, "Spectral and temporal characterization of a fused-quartz-microresonator optical frequency comb," Phys. Rev. A **84**(5), 053833–053839 (2011).
8. F. Ferdous, H. Miao, P. H. Wang, D. E. Leaird, K. Srinivasan, L. Chen, V. Aksyuk, and A. M. Weiner, "Probing coherence in microcavity frequency combs via optical pulse shaping," Opt. Express **20**(19), 21033–21043 (2012).
9. M. Fujiwara, M. Teshima, J. Kani, H. Suzuki, N. Takachio, and K. Iwatsuki, "Optical carrier supply module using flattened optical multicarrier generation based on sinusoidal amplitude and phase hybrid modulation," J. Lightwave Technol. **21**(11), 2705–2714 (2003).

#182353 - $15.00 USD Received 27 Dec 2012; revised 14 Feb 2013; accepted 23 Feb 2013; published 4 Mar 2013

10. T. Yamamoto, T. Komukai, K. Suzuki, and A. Takada, "Multicarrier light source with flattened spectrum using phase modulators and dispersion medium," J. Lightwave Technol. **27**(19), 4297–4305 (2009).
11. R. Wu, V. R. Supradeepa, C. M. Long, D. E. Leaird, and A. M. Weiner, "Generation of very flat optical frequency combs from continuous-wave lasers using cascaded intensity and phase modulators driven by tailored radio frequency waveforms," Opt. Lett. **35**(19), 3234–3236 (2010).
12. K. Imai, M. Kourogi, and M. Ohtsu, "30-THz span optical frequency comb generation by self-phase modulation in an optical fiber," J. Lightwave Technol. **34**(1), 54–60 (1998).
13. I. Morohashi, T. Sakamoto, H. Sotobayashi, T. Kawanishi, and I. Hosako, "Broadband wavelength-tunable ultrashort pulse source using a mach-zehnder modulator and dispersion-flattened dispersion-decreasing fiber," Opt. Lett. **34**(15), 2297–2299 (2009).
14. C. B. Huang, S. G. Park, D. E. Leaird, and A. M. Weiner, "Nonlinearly broadened phase-modulated continuous-wave laser frequency combs characterized using DPSK decoding," Opt. Express **16**(4), 2520–2527 (2008).
15. V. R. Supradeepa and A. M. Weiner, "Bandwidth scaling and spectral flatness enhancement of optical frequency combs from phase-modulated continuous-wave lasers using cascaded four-wave mixing," Opt. Lett. **37**(15), 3066–3068 (2012).
16. K. Tamura, H. Kubota, and M. Nakazawa, "Fundamentals of stable continuum generation at high repetition rates," J. Lightwave Technol. **36**(7), 773–779 (2000).
17. Y. Takushima and K. Kikuchi, "10-GHz, over 20-channel multiwavelength pulse source by slicing super-continuum spectrum generated in normal-dispersion fiber," IEEE Photon. Technol. Lett. **11**(3), 322–324 (1999).
18. F. Parmigiani, C. Finot, K. Mukasa, M. Ibsen, M. A. Roelens, P. Petropoulos, and D. J. Richardson, "Ultra-flat SPM-broadened spectra in a highly nonlinear fiber using parabolic pulses formed in a fiber Bragg grating," Opt. Express **14**(17), 7617–7622 (2006).
19. A. Clarke, D. Williams, M. Roelens, and B. Eggleton, "Reconfigurable optical pulse generator employing a fourier-domain programmable optical processor," IEEE Photon. Technol. Lett. **28**(1), 97–103 (2010).
20. X. Yang, D. J. Richardson, and P. Petropoulos, "Nonlinear generation of ultra-flat broadened spectrum based on adaptive pulse shaping," J. Lightwave Technol. **30**(12), 1971–1977 (2012).
21. K. Kashiwagi, H. Ishizu, Y. Kodama, S. Choi, and T. Kurokawa, "Highly precise optical pulse synthesis for flat spectrum supercontinuum generation with wide mode spacing," in *European Conference on Optical Communication (ECOC),* We.7.E.5 (2010).
22. A. M. Weiner, "Femtosecond pulse shaping using spatial light modulators," Rev. Sci. Instrum. **71**(5), 1929–1960 (2000).
23. H. Tsuda, Y. Tanaka, T. Shioda, and T. Kurokawa, "Analog and digital optical pulse synthesizers using arrayed-waveguide gratings for high-speed optical signal processing," J. Lightwave Technol. **26**(6), 670–677 (2008).
24. Y. Tanaka, R. Kobe, T. Kurokawa, T. Shioda, and H. Tsuda, "Generation of 100-Gb/s packets having 8-bit return-to-zero patterns using an optical pulse synthesizer with a lookup table," IEEE Photon. Technol. Lett. **21**(1), 39–41 (2009).
25. R. Wu, C. M. Long, D. E. Leaird, and A. M. Weiner, "Directly generated Gaussian-shaped optical frequency comb for microwave photonic filtering and picosecond pulse generation," IEEE Photon. Technol. Lett. **24**(17), 1484–1486 (2012).
26. V. Torres-Company, J. Lancis, and P. Andrés, "Lossless equalization of frequency combs," Opt. Lett. **33**(16), 1822–1824 (2008).
27. J. Azana, "Time-to-frequency conversion using a single time lens," Opt. Commun. **217**(1–6), 205–209 (2003).
28. J. van Howe and C. Xu, "Ultrafast optical signal processing based upon space-time dualities," J. Lightwave Technol. **24**(7), 2649–2662 (2006).
29. V. Torres-Company, J. Lancis, and P. Andres, "Space-time analogies in optics," Prog. Opt. **56**, 1–80 (2011).
30. V. R. Supradeepa, C. M. Long, R. Wu, F. Ferdous, E. Hamidi, D. E. Leaird, and A. M. Weiner, "Comb-based radiofrequency photonic filters with rapid tunability and high selectivity," Nat. Photonics **6**(3), 186–194 (2012).
31. M. Song, V. Torres-Company, A. J. Metcalf, and A. M. Weiner, "Multitap microwave photonic filters with programmable phase response via optical frequency comb shaping," Opt. Lett. **37**(5), 845–847 (2012).
32. M. Song, R. Wu, V. Torres-Company, D. E. Leaird, and A. M. Weiner, "Programmable microwave photonic phase filters with large time-bandwidth product based on ultra-broadband optical frequency comb generation," in *Microwave Photonics (MWP), 2012 IEEE Topical Meeting* (2012).
33. V. R. Supradeepa, C. M. Long, D. E. Leaird, and A. M. Weiner, "Self-referenced characterization of optical frequency combs and arbitrary waveforms using a simple, linear, zero-delay implementation of spectral shearing interferometry," Opt. Express **18**(17), 18171–18179 (2010).
34. G. P. Agrawal, *Nonlinear Fiber Optics*, 4th ed. (Academic, 2007).
35. C. Finot, B. Kibler, L. Provost, and S. Wabnitz, "Beneficial impact of wave-breaking for coherent continuum formation in normally dispersive nonlinear fibers," J. Opt. Soc. Am. B **25**(11), 1938–1948 (2008).
36. W. J. Tomlinson, R. H. Stolen, and A. M. Johnson, "Optical wave breaking of pulses in nonlinear optical fibers," Opt. Lett. **10**(9), 457–459 (1985).
37. Y. Liu, H. Tu, and S. A. Boppart, "Wave-breaking-extended fiber supercontinuum generation for high compression ratio transform-limited pulse compression," Opt. Lett. **37**(12), 2172–2174 (2012).
38. J. P. Heritage, R. N. Thurston, W. J. Tomlinson, A. M. Weiner, and R. H. Stolen, "Spectral windowing of frequency-modulated optical pulses in a grating compressor," Appl. Phys. Lett. **47**(2), 87–89 (1985).
39. A. M. Weiner, *Ultrafast Optics* (Wiley, 2009), Chap. 3.

#182353 - $15.00 USD Received 27 Dec 2012; revised 14 Feb 2013; accepted 23 Feb 2013; published 4 Mar 2013

1. Introduction

Optical frequency combs with a high degree of coherence, excellent spectral flatness, stability, as well as a broad bandwidth at high repetition rates are desirable for various applications such as wavelength division multiplexing [1], optical orthogonal frequency division multiplexing [2], and optical arbitrary waveform generation [3].

The most recent efforts to generate very broad optical frequency combs with high repetition rates in the range of 10 to 1,000 GHz involve the use of parametric frequency conversion in ultrahigh-quality-factor monolithic microresonators [4] or cascaded highly nonlinear fibers (HNLF) [5]. Although very promising due to the huge spectral bandwidth, these approaches do not provide the high degree of flatness [4] or reconfiguration flexibility [5] required by some mentioned applications. Furthermore, the microring-resonator based combs may be temporally partially coherent which limits the performance in, e.g. short pulse generation [6–8].

Alternatively, a more established approach to generate optical frequency combs with repetition rates up to tens of GHz is by employing cascaded electro-optic modulators [9–11]. This approach is very versatile because the comb's repetition rate can be continuously tuned independently of the optical center frequency. Unfortunately the efficiency of the electro-optic modulation limits the resulting bandwidth to several nanometers at best without compromising the complexity of the setup. Instead, one can use nonlinear optics to achieve further broadening [12–14]. This has been reported using dispersion-flattened fiber [12] or dispersion decreasing fiber [13,14]. However, typical electro-optic frequency comb generators are configured to provide a relatively flat optical spectrum, and the corresponding sinc-like temporal profile is far from optimum to preserve the flatness while achieving the broadening [13,14]. Reference [15] is an exception, in which the comb bandwidth is broadened while keeping the flat-topped comb profile based on a cascaded four-wave mixing scheme in a length of HNLF with near zero dispersion. However to increase the flat comb bandwidth to >10 nm is experimentally very challenging.

Prior investigations in spectral broadening of high-rep-rate temporal pulse trains from actively mode-locked lasers [16–20] or electro-optic frequency comb generator [21] showed a high degree of flatness with broad bandwidth when sech [17,18], parabolic [18,19] or Gaussian [20,21] profile pulses are launched into an HNLF operating in the normal dispersion regime. However, achieving this kind of temporal pulse shapes directly (i.e., without optical pre-shaping [21–24]) from an electro-optic frequency comb generator has remained challenging. Recently, we have shown the synthesis of a Gaussian-shaped comb [25] using the concepts of time-to-frequency mapping [26–29]. Here, we show that the temporal profile emerging from this comb can be used as a seed to achieve an ultra-broad optical spectrum (> 3.64-THz or 28-nm) with excellent flatness (more than 365 lines within 3.5 dB power variation) and a high-degree of coherence. To illustrate the high-degree of stability and coherence of the source, we demonstrate pulse compression to the transform-limited duration.

2. System setup and results

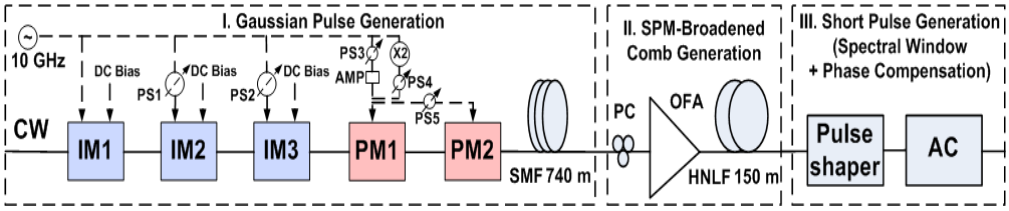

Fig. 1. Experimental scheme to generate supercontinuum flat-topped comb and the application for high quality temporal pulse compression. CW: continuous wave; IM: intensity modulator; PM: phase modulator; PS: phase shifter; AMP: RF amplifier; SMF: single-mode fibers; PC: polarization controller; OFA: Er-Yb-doped optical fiber amplifier; HNLF: highly nonlinear fiber; AC: autocorrelator.

#182353 - $15.00 USD Received 27 Dec 2012; revised 14 Feb 2013; accepted 23 Feb 2013; published 4 Mar 2013

Figure 1 shows the system setup to generate super-continuum flat-topped optical comb and the application for high-quality short-pulse compression. The whole setup is composed of three subsystems as follows:

2.1. Gaussian pulse generation

The first part of Fig. 1 explains our Gaussian-shaped comb generation scheme [25]. Briefly, the synthesis concept is based on time-to-frequency mapping theory, where quadratic and periodic temporal phase causes the spectral envelope generated at the output of the phase modulators to mimic the input intensity profile [26–29]. The Gaussian comb is generated by cascading three intensity modulators (IMs) for gating Gaussian pulses and two phase modulators (PMs). The PMs are driven by a "quasi-quadratic" temporal signal, which is formed by combining the first and second harmonics from an RF oscillator with an appropriate power ratio which improves the approximation to the target quadratic phase profile [25], resulting in significantly improved time-to-frequency mapping [11]. By cascading two phase modulators driven at their maximum RF input power (30 dBm), we double the total modulation index seen by the gated Gaussian pulse and double the number of comb lines. The RF oscillator in our experiments is set to 10 GHz, which determines the repetition rate of the comb to 10 GHz. At 10 GHz, V_π is ~9 V for the IM's and ~3 V for the PM's. IM1 and IM2 are both biased at 0.5 V_π with RF drive amplitude 0.5 V_π. IM3 is biased at the maximum transmission point with RF drive amplitude V_π .

We note that to scale the scheme presented here to substantially beyond the current 10 GHz repetition rate raises practical challenges, both because of the need for the frequency doubler circuit itself and because the phase modulators must have a bandwidth equal to twice the repetition frequency. Our group has recently demonstrated similar improvements in the comb spectrum by exploiting four-wave-mixing in HNLFs and achieved ultraflat [15] or Gaussian-like [30] optical frequency comb generators without the use of a frequency doubler. These related schemes may be better suited for scaling to higher repetition rates. The 10 GHz repetition rate demonstrated here is already sufficiently high for application to comb-based RF photonics amplitude [25] and phase [31,32] filters.

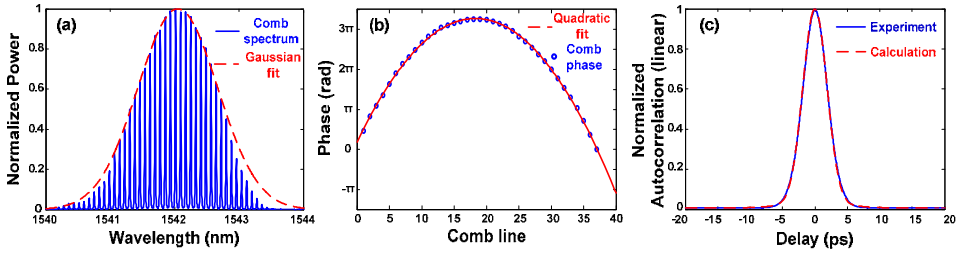

Fig. 2. Experimental results [25]. (a) Experimentally measured optical spectrum of the frequency comb generated from Fig. 1 (blue) with Gaussian fit (red); (b) Experimentally measured comb phase (blue) with quadratic fit (red) vs. comb line number which increases in wavelength; (c) Normalized intensity autocorrelation (blue) of the output pulse after comb propagation through 750 m of SMF and calculation (red) based on the comb spectrum in (a) assuming a flat phase on a linear scale.

Figure 2(a) shows the optical spectrum of the output comb, which has ~40 lines, and whose shape agrees very well with a Gaussian fit. The power in the central 23 lines matches within a standard deviation of 2% to an ideal Gaussian shape. Figure 2(b) shows the spectral phase of the comb (blue) vs. comb line number which increases in wavelength measured using a linear optical implementation of spectral shearing interferometry [33]. The phase has quadratic profile (red), as expected. This indicates that pulse compression can be accomplished using the appropriate length of single-mode fiber (SMF). The blue solid curve in Fig. 2(c) shows on a linear scale the measured intensity autocorrelation of the output pulse after passing the comb in Fig. 2(a) through 740 meter of SMF. The theoretical intensity

#182353 - $15.00 USD Received 27 Dec 2012; revised 14 Feb 2013; accepted 23 Feb 2013; published 4 Mar 2013

autocorrelation (red dashed curve) taking into account the measured comb spectrum and assuming a flat phase is plotted as well. The excellent agreement between the two curves indicates high-quality pulse compression to the bandwidth-limit duration. The measured autocorrelation trace shown in Fig. 2(c) has 4.35 ps full width at the half maximum (FWHM), corresponding to a deconvolved 3.1 ps pulse width assuming a Gaussian pulse shape.

2.2. SPM-Broadened flat-topped supercontinuum comb generation

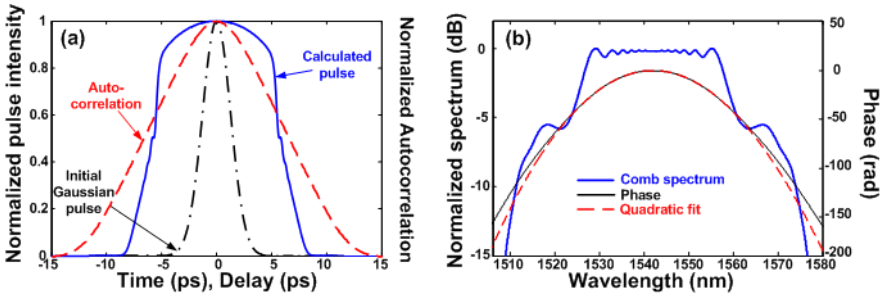

Fig. 3. Simulation results (a) Propagating Gaussian pulse in 150 m HNLF with 1.7 W average power. Initial pulse with 3-ps FWHM (black), output pulse (blue) and corresponding autocorrelation trace (red); (b) Output optical spectrum envelope (blue) and phase (black) with quadratic fit (red).

Next, in order to perform spectral broadening, the transform-limited Gaussian pulse was amplified with an Er-Yb-doped optical fiber amplifier (OFA) and fed into 150 meters of HNLF with dispersion −1.88 ps/nm/km (as specified by the manufacturer), nonlinear coefficient of 10 $(W\bullet km)^{-1}$ and fiber attenuation of 0.22 dB/km as shown in the second part of Fig. 1. Figure 3 shows our simulation results from solving the nonlinear Schrödinger equation using the split-step Fourier method [34]. For a qualitative study, we simulate the initial input pulse as a single perfect Gaussian-shaped profile with 3-ps FWHM as shown in black dotted trace of Fig. 3(a). The blue trace in Fig. 3(a) shows the output broadened pulse. Figure 3(b) shows the simulated output comb spectrum envelope (blue) and phase (red) with quadratic fit (black). The spectral phase has a quadratic profile within the turning points of the shoulders of the comb spectrum. From a practical perspective, a specific length of SMF can be used to compensate for most of the spectral phase. Figure 4 shows the experimental output ultra-broadband flat-topped optical frequency comb spectrum when we tune the power of the OFA to 1.7 Watt. This comb shows excellent broadening and a flatness corresponding to 3.5 dB variation over 3.64 THz (28 nm or 365 lines), similar to the simulation prediction in Fig. 3(b). The characteristics of this comb source are promising for the realization of high-performance microwave photonic filters [30], where the ultimate limit in the achievable time-bandwidth product is directly proportional to the number of comb lines. This supercontinuum comb has already been demonstrated to be a promising source for such applications, with excellent stability in spectral amplitude, a large number of comb lines, and a broad bandwidth contributing to programmable microwave photonic phase filters with record time-bandwidth product [32].

We note that regions of the simulated intensity profile of Fig. 3(a) exhibit a nearly vertical rise or fall. Furthermore, the simulated and experimental spectra, Figs. 3(b) and 4, respectively, show clear spectral sidelobes on either side of the flat-topped central region. These observations are indicators that the pulse has entered into the wave-breaking regime [34–36]. This nonlinear phenomenon has been exploited as a route to achieve smooth and broad spectra with a high degree of stability [35] when pumped with bell-shaped pulses, and is gaining increasing popularity for applications requiring high-quality ultrashort-pulse compression [37]. Our experiments indicate that this phenomenon can also take place in the high-repetition-rate regime and is indeed suitable for applications involving electro-optic frequency comb generators.

#182353 - $15.00 USD Received 27 Dec 2012; revised 14 Feb 2013; accepted 23 Feb 2013; published 4 Mar 2013

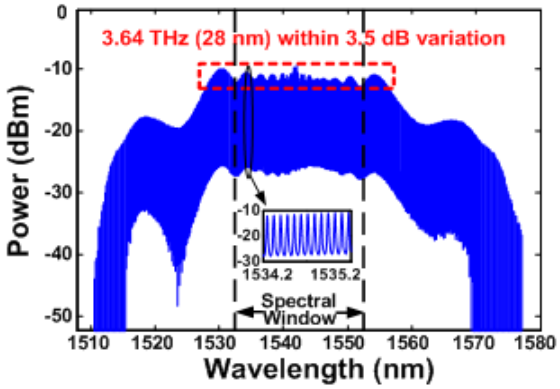

Fig. 4. Experimental optical power spectrum after propagation in 150-m HNLF with 1.7-W pulse average power before HNLF measured with 0.01nm OSA resolution. A spectral window, equivalent to a bandpass filter, keeps the center spectrum with linear chirp.

We have also performed measurements – at a lower average power level (0.75 W) – to test the stability of the comb. Figure 5 (a) shows the simulated optical spectrum (blue) with spectral phase (black) and quadratic fit (red) at 0.75 W average power. Comparing with the simulated comb spectrum at 1.7 W average power in Fig. 3(b), the comb bandwidth in Fig. 5(a) is somewhat decreased due to the reduced pump power. We repeatedly measured the comb spectrum using an OSA set for 0.01 nm spectral resolution, recording 14 spectra over a period of approximately 70 minutes. The output comb spectrum has 237 lines (18.6 nm or 2.36 THz) within 4.5 dB power variation as shown in Fig. 5(b). Figure 5(c) provides data on the stability of each of the individual comb lines over this data set. Most of the comb lines have variations with standard deviation below 0.1 dB. The average and median standard deviations of all the comb line variations are 0.08 dB and 0.09 dB, respectively. The largest fluctuations are observed for the four lines closest to the input CW laser (1542 nm), with a standard deviation ranging from 0.35 dB to 0.66 dB. Overall, this indicates the stability of this comb source can be very good.

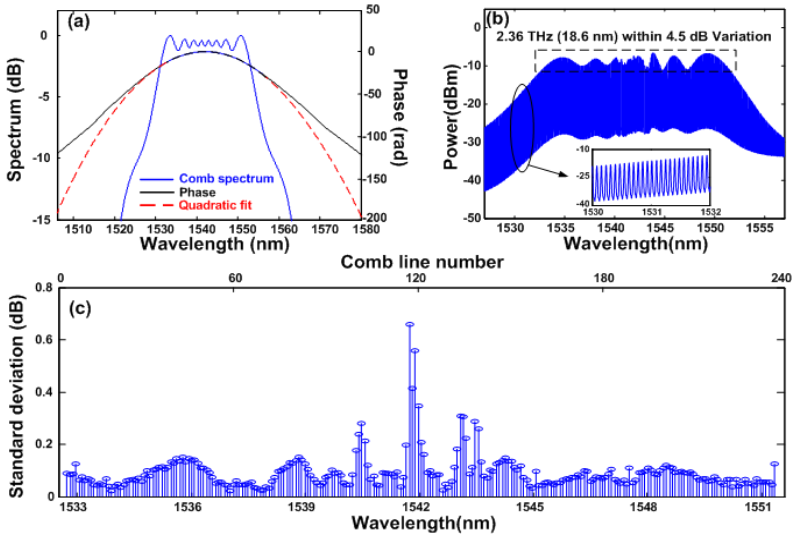

Fig. 5. Stability analysis: (a) Simulated optical spectrum (blue) with spectral phase (black) and quadratic fit (red) at 0.75 W average power. (b) Optical spectrum measured with 0.01nm OSA resolution. (c) Stability analysis which shows spectral amplitude standard deviation of each comb line versus the number of comb line and wavelength after approximately 70 minutes of measurements.

#182353 - $15.00 USD Received 27 Dec 2012; revised 14 Feb 2013; accepted 23 Feb 2013; published 4 Mar 2013

2.3. Application for short pulse compression

Maintaining a high degree of coherence across the entire bandwidth of the supercontinuum obtained by picosecond pump pulses is challenging [16]. According to a previous study, the situation improves when the HNLF is designed to have a normal dispersion profile [14], since the amplification of input noise due to modulation instability is avoided. Thus, apart from offering a smooth and broad spectrum, an HNLF with normal dispersion should provide a supercontinuum with high degree of coherence too. In order to demonstrate the high quality of our broadened comb as well as the spectral stability, we perform a pulse compression experiment in this section. The broad supercontinuum was attenuated by 10-dB and sent to a commercial pulse shaper (FinisarWaveshaper 1000S), as indicated in Fig. 1. The output from the shaper was measured with an autocorrelation apparatus. When the pulse shaper was programmed as an all-pass filter, the autocorrelation trace has a roughly triangular shape, much broader than the initial Gaussian pulse [black dotted trace in Fig. 6(a)] before the HNLF. The approximately triangular autocorrelation is roughly as expected for the flat-topped intensity profile predicted in the nonlinear wave-breaking regime in Fig. 3. The slight narrowing of the experimental autocorrelation trace (Fig. 6(a)) relative to the simulated one (Fig. 3(a)) is attributed to the dispersion in the short SMF between HNLF and the pulse shaper. From Fig. 3(b), one can conclude that the central part of the spectrum can be easily compensated for by introducing the right amount of dispersion. In order to compensate for the comb phase, we first programmed the pulse shaper to apply the amount of quadratic spectral phase that maximized the second-harmonic generation (SHG) at the zero delay position of the autocorrelation setup. Figure 6(b) shows the measured autocorrelation trace (blue) with very large pedestal. Similar to what was observed in [18], the measured trace does not match the calculated autocorrelation based on the input comb spectrum assuming a flat phase. An explanation is that the outer part of the spectrum, as shown in the simulation of Fig. 3(b), deviates from quadratic phase. To overcome this limitation, we programmed the pulse shaper to apply a spectral window [38] that selects the central 20 nm of the supercontinuum comb as shown in Fig. 4. In this region the phase remains approximately quadratic and the spectrum maintains an approximately rectangular profile. Again we programmed the pulse shaper to apply the amount of quadratic spectral phase that maximized the SHG at the zero delay position. The autocorrelation now shows a high-quality pedestal-free trace as shown in the blue curve of Fig. 6(c), which has an excellent correspondence with the calculated one taking into account the measured spectrum after windowing and assuming a flat spectral phase. The ability to achieve pulse compression to the transform-limit indicates a high degree of coherence across the comb spectrum –i.e., the relative phase of the different comb lines do not vary significantly in time [39]. The autocorrelation width is 533 fs FWHM. To estimate the actual pulse width, we calculate the transform-limited intensity profile and estimated its width to be 490 fs FWHM, as shown in Fig. 6(d).

#182353 - $15.00 USD Received 27 Dec 2012; revised 14 Feb 2013; accepted 23 Feb 2013; published 4 Mar 2013

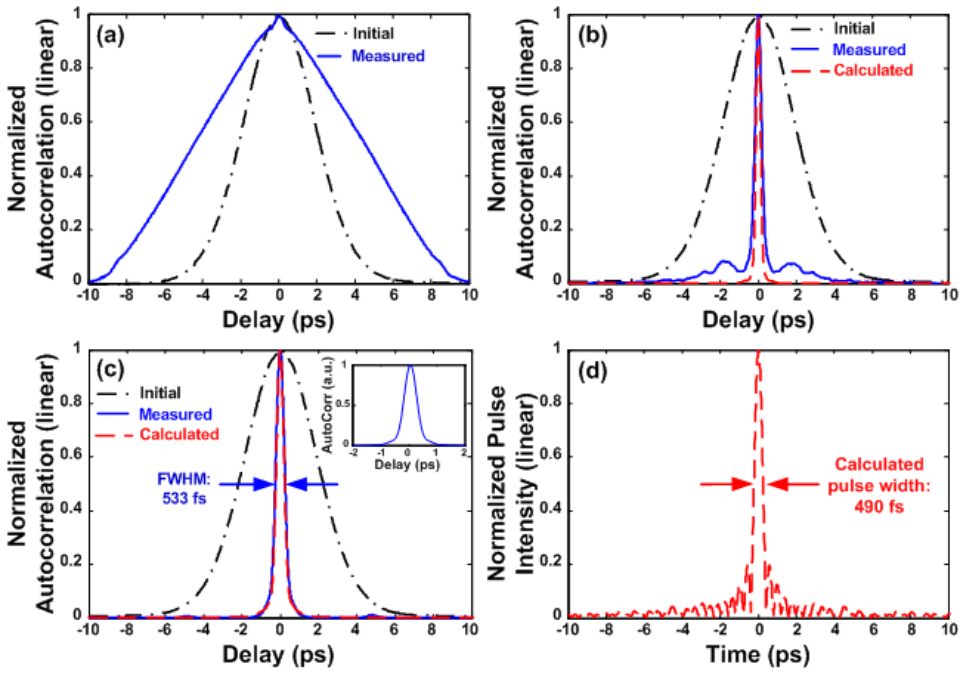

Fig. 6. Application of the flat-topped super-continuum comb for short pulse compression. Measured autocorrelation traces of the initial Gaussian pulse, after compression, at the output of the first box in Fig. 1 shown as black traces in (a)-(c)); (a) Blue trace: measured autocorrelation trace of pulse with the whole spectrum of super-continuum comb without phase compensation; (b) blue trace: measured autocorrelation trace of pulses with the whole spectrum of super-continuum comb after quadratic phase compensation; red trace: calculated autocorrelation trace with the input super-continuum comb assuming a flat phase; (c) blue trace: measured autocorrelation trace of pulse with the truncated spectrum of super-continuum comb after quadratic phase compensation; red trace: calculated autocorrelation trace with the truncated super-continuum comb assuming a flat phase. An excellent agreement between the experimental and simulated autocorrelation traces indicates accurate spectral phase compensation. Inset is the zoom-in of measured pulse autocorrelation trace. The corresponding pulse shape is calculated in (d).

3. Conclusion

In summary, we have generated a flat-topped optical frequency comb at 10-GHz repetition rate covering the whole C-band with >3.64 THz or ~365 lines within 3.5 dB power variation by seeding a directly generated 3.1-ps Gaussian pulse train from an electro-optic modulated comb followed by a HNLF in the normal dispersion regime. The combination of broad bandwidth, flatness and the demonstrated high degree of coherence should enable further applications in ultrafast photonics such as microwave photonic phase filters [31,32], for which the accurate synthesis of optical waveforms with a large time-bandwidth product is of paramount importance.

Acknowledgment

This project was supported in part by the Naval Postgraduate School under grant N00244-09-1-0068 under the National Security Science and Engineering Faculty Fellowship program and by the National Science Foundation under grant ECCS-1102110. Any opinion, findings, and conclusions or recommendations expressed in this publication are those of the authors and do not necessarily reflect the views of the sponsors. Victor Torres-Company gratefully acknowledges funding from the Swedish Research Council (VR).